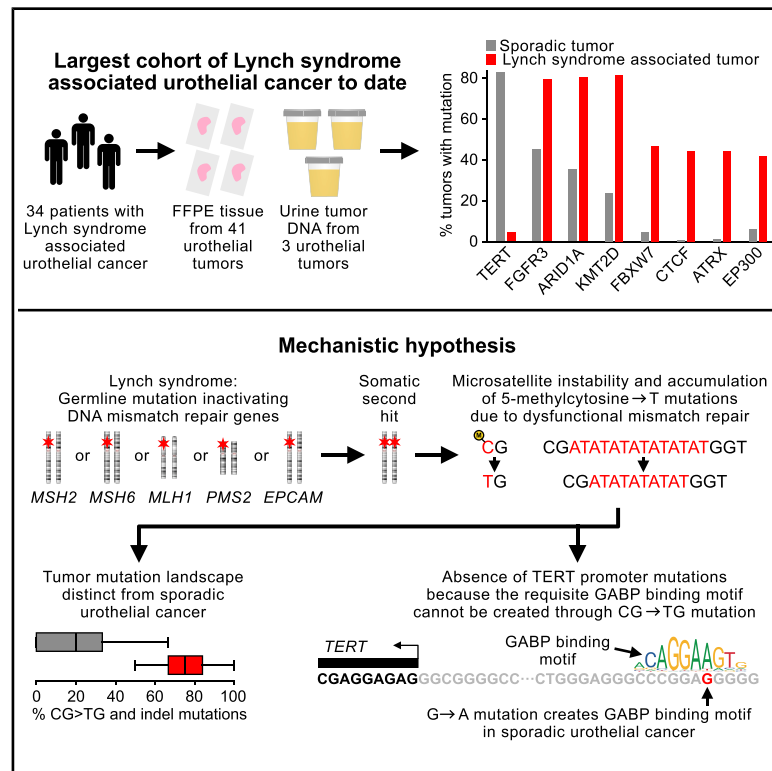


Constrained hypermutation and absence of *TERT* promoter mutations in Lynch syndrome-associated urothelial cancer

Graphical abstract



Authors

Jussi Nikkola, Lauri Ryyppö, Juuso Vuorinen, ..., Jukka-Pekka Mecklin, Toni T. Seppälä, Matti Annala

Correspondence

jussi.nikkola@fimnet.fi (J.N.), matti.annala@tuni.fi (M.A.)

In brief

Nikkola et al. demonstrate that Lynch syndrome-associated urothelial cancers are mismatch-repair deficient and evolve through a mutagenic process dominated by 5-methylcytosine deamination and microsatellite instability. This results in a distinct mutational landscape marked by the absence of *TERT* promoter mutations and near-universal mutation of *ARID1A*, *FGFR3*, and *KMT2D*.

Highlights

- Lynch syndrome-associated urothelial cancers (LS-UCs) have a unique mutation landscape
- All LS-UC genomes show evidence of bi-allelic DNA mismatch repair defect
- *TERT* promoter mutations are almost completely absent in LS-UC
- LS-UC-dominant mutagenic processes cannot create GABP binding motifs at *TERT* promoter



Report

Constrained hypermutation and absence of *TERT* promoter mutations in Lynch syndrome-associated urothelial cancer

Jussi Nikkola,^{1,2,8,*} Lauri Ryyppö,^{1,8} Juuso Vuorinen,^{1,8} Lauri Moilanen,³ Maarit Ahtiainen,³ Kirsi Pylvänäinen,⁴ Hanna Selin,¹ Tuomo Virtanen,¹ Matti Nykter,¹ Thea Veitonmäki,² Jukka-Pekka Mecklin,^{4,5} Toni T. Seppälä,^{1,6,7,9} and Matti Annala^{1,9,10,*}

¹Faculty of Medicine and Health Technology, Tampere University and Tays Cancer Centre, Tampere, Finland

²Department of Urology, Tampere University Hospital, Tampere, Finland

³Department of Pathology, Hospital Nova of Central Finland, Jyväskylä, Finland

⁴Department of Education and Research, The Wellbeing Services County of Central Finland, Jyväskylä, Finland

⁵Faculty of Sport and Health Sciences, University of Jyväskylä, Jyväskylä, Finland

⁶Applied Tumor Genomics, Research Programs Unit and Abdominal Center, University of Helsinki, Helsinki, Finland

⁷Department of Gastroenterology and Alimentary Tract Surgery, Tampere University Hospital, Tampere, Finland

⁸These authors contributed equally

⁹These authors contributed equally

¹⁰Lead contact

*Correspondence: jussi.nikkola@fimnet.fi (J.N.), matti.annala@tuni.fi (M.A.)

<https://doi.org/10.1016/j.celrep.2025.116388>

SUMMARY

Lynch syndrome (LS) is a hereditary condition characterized by defective DNA mismatch repair and a high incidence of several cancers. In this study, we investigate the somatic landscape of LS-associated urothelial cancer (LS-UC) by analyzing 41 tumor and 3 urine samples from 34 patients with LS-UC. We show that telomerase reverse transcriptase (*TERT*) promoter mutations found in 83% of sporadic UC are almost absent (5%) in LS-UC. Instead, LS-UC carries a 5-methylcytosine-deamination- (CG>TG) and microsatellite-instability-driven mutation landscape characterized by frequent *ARID1A* (82%), *FGFR3* (80%), and *KMT2D* (81%) mutations. We propose that the scarcity of *TERT* promoter mutations in LS-UC is due to the inability to create the GA-binding protein (GABP) binding motif 5'-GGAA through CG>TG mutations or microsatellite instability. Our data demonstrate that LS-UC represents a disease entity with unique genomic characteristics relevant for diagnosis and screening, and represents the largest analysis to date of the LS-UC mutation landscape.

INTRODUCTION

Lynch syndrome (LS) is a dominantly inherited cancer predisposition syndrome characterized by inactivating germline mutations in the DNA mismatch repair (MMR) genes *MSH2*, *MSH6*, *MLH1*, or *PMS2*, or *EPCAM* deletions that lead to *MSH2* silencing.¹ Affected patients suffer from a high incidence of colon and endometrial cancer but also a 10%–25% lifetime risk of urothelial cancer (UC), particularly in the upper urinary tract.² LS-associated cancers typically obtain an inactivating second hit to the predisposing gene during early tumorigenesis.³ The second hit disrupts DNA repair, resulting in accelerated mutagenesis, with particular enrichment of CG>TG mutations arising from spontaneous 5-methylcytosine deamination, and changes to microsatellite lengths.⁴

The most common somatic genomic alteration in sporadic UC is mutation of the telomerase reverse transcriptase (*TERT*) promoter, occurring at one of two mutation hotspots (–124C>T or –146C>T) in 70%–80% of patients.⁵ These mutations increase *TERT* expression by creating a GA-binding protein

(GABP) transcription factor binding site with the core motif 5'-GGAA and are an early event in tumorigenesis.⁶ *TERT* plays a key role in telomere elongation, and its overexpression enhances this activity.⁷ Sporadic UC tumors also harbor recurrent mutations in *FGFR3*, *TP53*, *PIK3CA*, *KDM6A*, *ERBB2*, *ERBB3*, and *STAG2*.⁸ A study by Donahue et al. provided early evidence that LS-associated UCs (LS-UCs) carry more mutations in several genes, including *FGFR3*, *ARID1A*, and *KMT2D*, but did not investigate the *TERT* promoter region and was restricted to a small cohort consisting solely of upper tract urothelial tumors (upper tract urothelial cancer [UTUC]).⁹ To investigate the tumorigenesis and genomic drivers of bladder cancer and UTUC in patients with LS, we set out to analyze a large, clinically representative cohort of biobanked LS-UC tumor tissue.

RESULTS

LS-UCs display bi-allelic MMR gene inactivation

We searched all UC diagnoses for patients in the Finnish Lynch Syndrome Registry and collected 41 UC surgical tissue



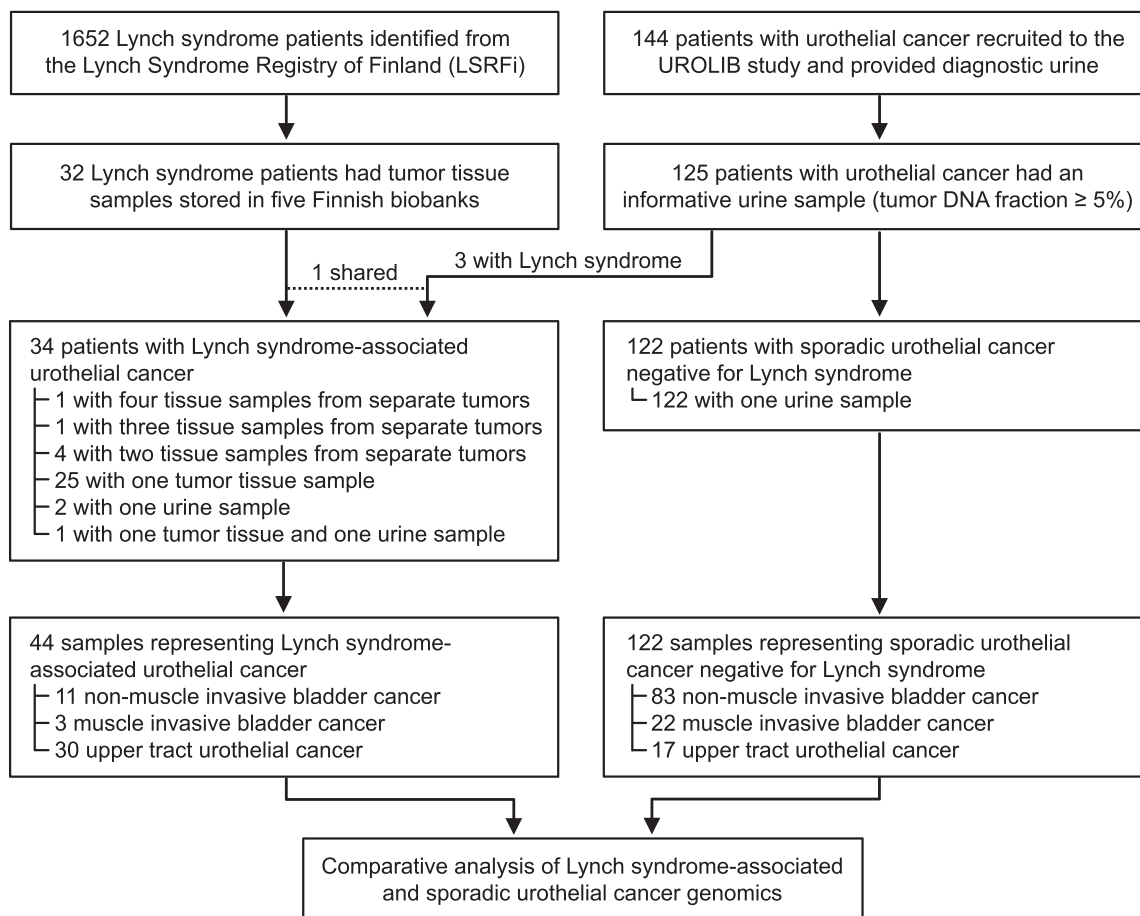


Figure 1. Consort diagram of the Lynch syndrome-associated urothelial cancer cohort and the sporadic urothelial cancer cohort

samples accrued to Finnish biobanks between April 1987 and June 2022 from a total of 32 patients with LS (22 UTUC and 10 bladder cancer without previous or subsequent UTUC diagnosis). We also analyzed 125 informative urine samples (cancer cell fraction $\geq 5\%$) collected between January 2021 and January 2024 from 122 patients with sporadic UC and 3 patients with LS-associated UTUC recruited to the UROLIB study (Table S1).¹⁰ In total, samples from 34 patients with LS-UC were analyzed (31 provided tissue, 2 provided urine, and 1 provided both) (Figure 1). All patients were confirmed carriers of a pathogenic germline MMR variant (16 *MSH2*, 13 *MLH1*, and 5 *MSH6*). Compared to sporadic UC, LS-UC cases were more often UTUC (68% vs. 14%, $p = 1.0e-10$; of which ureteral 67% vs. 29%, $p = 0.030$), young (median 62 vs. 74 years, $p = 3.0e-7$), and female (48% vs. 23%, $p = 0.0046$) (Table 1), consistent with prior literature.¹¹ UC was the first diagnosed cancer in 10 (29%) patients with LS-UC, while 13 (38%) had a prior colorectal cancer diagnosis, and 6 (18%) had a prior endometrial cancer diagnosis.

All tissue and urine samples were analyzed using the UroScout assay, a hybridization capture panel targeting 25 UC-associated genes, including the MMR genes¹⁰ (Table S2). The cancer cell fraction varied between 19% and 96% (median: 57%) in tumor

tissue samples and between 29% and 57% (median: 30%) in urine samples. A pathogenic germline MMR variant was detected in all patients with LS-UC, and a somatic second hit to the same gene was detected in 82% of cases (Table S1). Immunohistochemistry confirmed loss of the relevant MMR protein in all LS-UC tumor samples (Figure S1).

TERT mutations are rare in LS-UC

To investigate LS-UC tumorigenesis, we characterized the somatic mutation landscape of LS-UC and sporadic UC samples using the UroScout panel and compared gene mutation frequencies (Figure 2A). *TERT* gene promoter mutations at the two classic mutation hotspots ($-124C>T$ and $-146C>T$) were detected in 101/122 (83%) sporadic UC tumors but only 2/44 (5%) LS-UC tumors ($p = 8.5e-21$, Fisher's exact test) (Figures 2B and 2C; Table S3). Analyzing the *TERT* upstream region, we found no mutations or rearrangements that produced a GABP binding motif in any LS-UC tumors, nor other recurrent mutations or rearrangements (Figure 2D). To validate the scarcity of *TERT* promoter mutations in LS-UC, we investigated an independent sequencing cohort by Fujii et al. and found a complete absence of *TERT* promoter mutations in all seven LS-UC tumors in their study.¹² In contrast, *FGFR3* and *ARID1A* were mutated in 80% and 82% of

Table 1. Clinical characteristics of the LS-UC and sporadic UC cohorts at the time of tumor sample collection (surgical tissue or urine tumor DNA for LS-UC and urine tumor DNA for the sporadic UC cohort)

Characteristic	LS-UC tumors (n = 44)	Sporadic UC tumors (n = 122)
Tumor subtype		
Non-muscle invasive bladder cancer	11 (25%)	83 (68%)
pTa low grade	1 (2%)	46 (38%)
pTa high grade	5 (11%)	23 (19%)
pT1	5 (11%)	13 (11%)
pTis	0 (0%)	1 (1%)
Muscle invasive bladder cancer	3 (7%)	22 (18%)
pT2	2 (5%)	17 (14%)
pT3	1 (2%)	1 (1%)
pT4	0 (0%)	4 (3%)
Upper tract urothelial carcinoma	30 (68%)	17 (14%)
pTa low grade	3 (7%)	1 (1%)
pTa high grade	7 (16%)	2 (2%)
pTis	1 (2%)	0 (0%)
pT1	6 (14%)	1 (1%)
pT2	8 (18%)	2 (2%)
pT3	4 (9%)	8 (7%)
pT4	1 (2%)	3 (2%)
Sex		
Male	23 (52%)	94 (77%)
Female	21 (48%)	28 (23%)
Age		
39–49 years	5 (11%)	3 (2%)
50–59 years	8 (18%)	7 (6%)
60–69 years	18 (41%)	25 (20%)
70–79 years	10 (23%)	53 (43%)
80–91 years	3 (7%)	34 (28%)
Hematuria		
Macroscopic hematuria	24 (55%)	104 (85%)
Microscopic hematuria	0 (0%)	1 (1%)
No hematuria	13 (30%)	17 (14%)
Unknown	7 (16%)	0 (0%)

LS-UC cases, respectively, a significantly elevated rate relative to sporadic UC (Figure 2B). *ARID1A* inactivation has been shown to increase *TERT* expression in human cell lines¹³ and may compensate for the lack of *TERT*-activating mutations in LS-UC.

To expand our analysis beyond the 25 genes covered by the UroScout panel, we performed additional whole-exome sequencing on 43 of the LS-UC tumors (one tumor failed whole-exome sequencing) and compared mutation frequencies against a published cohort of 2,463 advanced-stage sporadic UC tumors.⁸ Whole-exome analysis validated findings obtained with the UroScout panel and revealed enrichment of LS-UC

mutations in additional UC-associated genes: *KMT2D*, *FBXW7*, *CREBBP*, *KMT2C*, and *EP300* (Figure 2E). Investigating genes linked to telomere maintenance, we found *ATRX* mutations in 19/43 (44%) LS-UC tumors but no mutations in *DAXX*, *TRF1*, or *TRF2* and only one mutation in *POT1* (Table S4). Inactivation of *ATRX* has been linked to telomere lengthening in human cancers.¹⁴ Finally, we found recurrent mutations in *CTCF*—a gene involved in chromatin looping—in 19/43 (44%) LS-UC tumors (Figure 2E). LS-UC enriched genes displayed higher mutation rates than expected based on their coding sequence length and genome-wide mutation density, suggesting these mutations are under preferential selection during tumorigenesis (Figure 2F). However, the microsatellite density of individual genes may also contribute. Differences in gene mutation frequency were not explained by differences in anatomic location, sex, or age between LS-UC and sporadic UC cases (Figures S2–S4).

Constrained hypermutation explains the LS-UC somatic mutation landscape

To investigate the mechanisms underlying the unique mutation landscape of LS-UC tumors, we studied the nucleotide context of somatic mutations detected in the analyzed tumors. An enrichment of CG>TG and insertion or deletion (indel) mutations was found in all LS-UC cases relative to sporadic UC (75% vs. 22% of all mutations, $p = 3.8e-60$), implicating DNA MMR dysfunction as the primary driver of LS-UC tumorigenesis (Figure 3A; Table S3).

We propose that *TERT* promoter mutations are absent in LS-UC because the core GABP binding motif 5'-GGAA cannot be created via CG>TG mutation or microsatellite instability, resulting in tumorigenesis through alternative somatic driver alterations (Figures 3B and S5). A similar pattern of constrained evolution was evident in the LS-UC mutation landscapes of other driver genes, such as *FGFR3*, *PIK3CA*, and *TP53*, with recurrent mutations strongly favoring well-characterized CG>TG mutation hotspots and microsatellite indels instead of the ordinary mutation hotspots characteristic of sporadic UC ($p = 5.8e-4$) (Figure 3C). In particular, the vast majority of *FGFR3* mutations in LS-UC were R248C and G380R hotspot mutations instead of the S249C and Y373C mutations that dominate in sporadic UC ($p = 5.0e-4$, Fisher's exact test) (Figure 3C). A high rate of *FGFR3* R248C mutations has been previously reported in LS-associated UTUC,⁹ and our data indicate that the same holds true for LS-associated bladder cancer (Figure 3D). More generally, the mutation landscapes of LS-associated bladder and upper tract tumors displayed no statistically significant differences (Figure 3D). We also did not find any significant differences between the mutation profiles of LS-associated tumors of the renal pelvis or ureter (Figure S6). Taken together, these data show that constrained hypermutation shapes the tumorigenesis of LS-UC, resulting in a unique somatic landscape enriched for CG>TG mutations and depleted for typical sporadic UC somatic mutations, including a striking absence of *TERT* promoter mutations.

DISCUSSION

This study represents the largest analysis to date of the LS-UC somatic landscape. We demonstrate that LS-UC is characterized

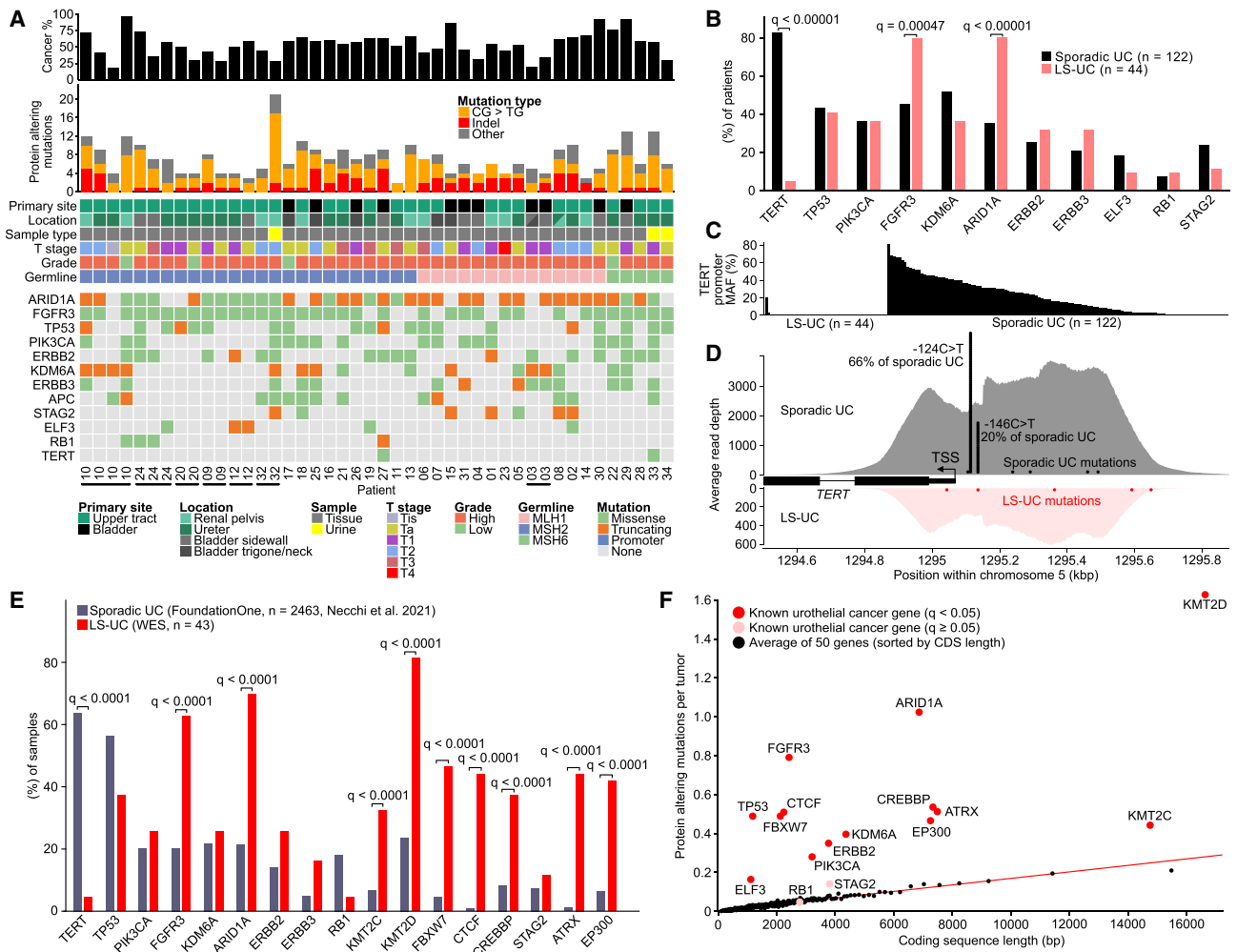


Figure 2. Somatic genomic landscape of Lynch syndrome-associated urothelial cancer

(A) Cohort overview and somatic mutation landscape. Same-patient tissue samples are indicated with horizontal underlines. Patients are sorted by the gene in which they harbored a germline DNA mismatch repair defect. The cancer cell fraction (cancer %) of tissue and urine samples is shown at the top. The primary site was defined as upper tract if the patient had any current or previous upper tract urothelial cancer diagnosis.

(B) Comparison of driver gene mutation frequency between sporadic and Lynch syndrome-associated urothelial cancer (LS-UC) tumors analyzed with the UroScout targeted sequencing assay. p values were calculated using Fisher's exact test and corrected for multiple hypothesis testing using the Benjamini-Hochberg procedure.

(C) Highest measured allele fraction for the two primary *TERT* promoter mutations in each sporadic and LS-UC sample. MAF, mutant allele fraction.

(D) Visualization of sequencing depth and detected mutations across the *TERT* promoter region in sporadic and LS-UC.

(E) Driver gene mutation frequencies in our LS-UC tissue cohort analyzed with whole-exome sequencing ($n = 43$) compared against published data from a large sporadic UC tissue cohort ($n = 2,463$) by Necchi et al.⁸ p values were calculated using Fisher's exact test and corrected for multiple hypothesis testing using the Benjamini-Hochberg procedure.

(F) Relationship between gene length and the frequency of protein-altering mutations in LS-UC tumors based on whole-exome sequencing. Genes were sorted by coding sequence (CDS) length and then combined into groups of 50 genes (dots). The mutation frequencies of known UC driver genes are indicated as large red dots. p values were calculated assuming a Poisson-distributed mutation count following the linear fit and corrected for multiple hypothesis testing using the Benjamini-Hochberg procedure.

by a unique mutation landscape, including an absence of *TERT* promoter mutations. Our hypothesis that *TERT* mutations are absent in LS-UC due to constrained hypermutation is supported by our observation that other UC driver genes exhibit a similarly altered mutation landscape in LS-UC. Most mutation hotspots that are recurrently mutated in sporadic UC were not mutated in LS-UC, with mutations instead

occurring at alternative hotspots with nucleotide contexts amenable to MMR-defect-driven hypermutation, particularly 5-methylcytosine deamination (CG>TG). The earlier age of onset and increased prevalence of UC in patients with LS, together with the high rate of somatic MMR loss of heterozygosity seen in LS-UC tumors, support a model in which LS-UC tumors arise via hypermutation after MMR loss of

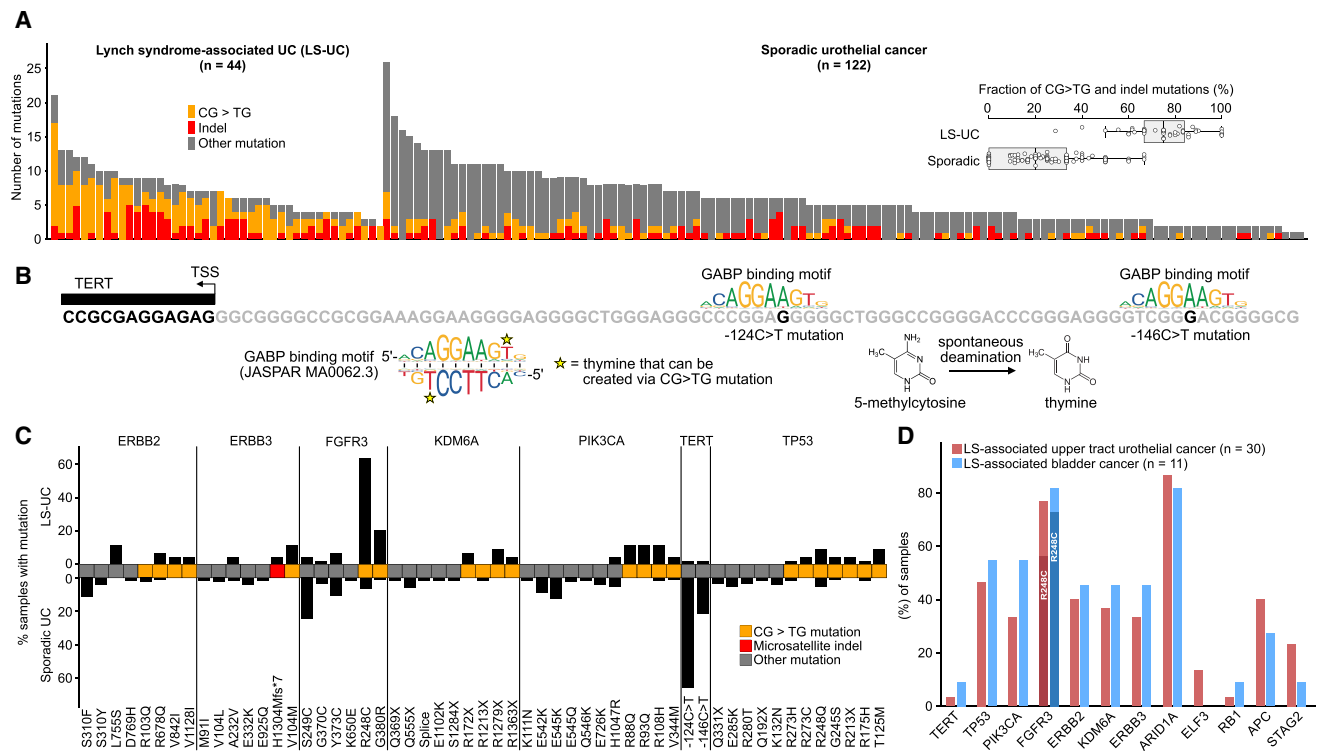


Figure 3. Constrained hypermutation shapes the tumorigenesis and somatic mutation landscape of Lynch syndrome-associated urothelial cancer

(A) Enrichment of CG>TG and indel-type somatic mutations in Lynch syndrome-associated urothelial cancer (LS-UC) relative to sporadic UC. (B) Visualization of the *TERT* upstream region and the GABP binding motifs created by the two most common *TERT* promoter mutations (–124C>T and –146C>T) in sporadic UC, neither of which can be created through CG>TG 5-methylcytosine deamination. In general, CG>TG mutations cannot produce the required 5'-GGAA GABP binding motif because the motif contains no TG dinucleotides. (C) Mutation frequency at recurrent mutation hotspots in sporadic UC and LS-UC. CG>TG, microsatellite indels, and other mutations are indicated using color. (D) Comparison of driver gene mutation frequency between LS-associated bladder cancers (11 tumors from 10 patients) and upper tract urothelial cancers (30 tumors from 24 patients) in our cohort. Patients that had prior or subsequent diagnosis of upper tract urothelial cancer were excluded from the bladder cancer group because of the high likelihood of drop seeding from the upper urothelial tract. The subset of *FGFR3* mutant samples with a p.R248C hotspot mutation is indicated using darker color. None of the genes displayed statistically significant differences ($p > 0.28$ for all, Fisher's exact test).

heterozygosity, and this nucleotide-context-constrained process of hypermutation circumvents the normal route of sporadic UC tumorigenesis through an alternative set of mutations. However, we cannot rule out contributions from alternative mechanisms, such as rapid tumorigenesis and young age of onset, resulting in a lower mitotic age for LS-UC tumors and a reduced need for *TERT* overexpression.

The distinct somatic landscape of LS-UC has clinical implications. The absence of *TERT* promoter mutations in LS-UC is relevant for existing commercial and in-development diagnostic tests relying on the detection of UC-associated DNA mutations.^{10,15,16} The high incidence of UC in patients with LS suggests that this population could benefit from non-invasive urine tumor DNA screening, a hypothesis investigated in our ongoing urine DNA screening study (ClinicalTrials.gov: NCT06218433). Patients with LS driven by an *MSH2* germline defect currently have a nearly equal risk of dying from UC (6%) as from colorectal cancer (9%), underscoring the need for effective screening strategies.² An accurate understanding of the LS-UC somatic mutation profile is important for DNA-based LS-UC screening. While immuno-

therapy remains the primary treatment option with excellent outcomes against MMR-defective tumors,¹⁷ the high prevalence of *FGFR* mutations in LS-UC suggests that intravesical or systemic fibroblast growth factor receptor (FGFR) inhibitors could be investigated as a therapeutic option in this patient population.

Limitations of the study

Our study provides no data on *TERT* activity at the RNA and protein levels, which limits our conclusions about the role of telomere maintenance in LS-UC tumorigenesis and the potential existence of alternative mechanisms of *TERT* activation or telomere maintenance. The cohort size, while the largest to date for LS-UC, remains relatively small, which limits the statistical power of subgroup analyses.

RESOURCE AVAILABILITY

Lead contact

All requests should be addressed to the lead contact, Matti Annala (matti.annala@tuni.fi).

Materials availability

This study did not generate any new unique reagents.

Data and code availability

The raw sequencing data generated in this study have been deposited into the European Genome-Phenome Archive (EGA) under study accession EGA: EGAD50000001220.

ACKNOWLEDGMENTS

This work was funded by research grants from the Jane and Aatos Erkko Foundation; the Research Council of Finland Center of Excellence Program (project 312043); the Finnish Cultural Foundation; the iCANDOC Doctoral Education Pilot in Precision Cancer Medicine, Research Council of Finland (project 359391); the Finnish Medical Foundation; the Orion Research Foundation; the Sigrid Jusélius Foundation; the Relander Foundation; the Cancer Society of Finland; the iCAN Precision Medicine Flagship of the Academy of Finland; and Competitive State Research Funding of Helsinki University Hospital and Tampere University Hospital. The sponsors had no role in the design and conduct of the study, data collection, data analysis, data interpretation, manuscript preparation, or approval of the manuscript. The authors wish to acknowledge the Biocenter Finland (BF) and Tampere Genomics Facility for their service, the CSC – IT Center for Science (Finland) for computational resources, and Nouscom for financially supporting whole-exome sequencing. The study benefited from samples from the Helsinki, Tampere, Auria, Central Finland, Eastern Finland, and Northern Finland biobanks. We are grateful to all participating patients and their families.

AUTHOR CONTRIBUTIONS

J.N., M. Annala, T.T.S., and J.-P.M. designed and supervised the study. J.V. and H.S. handled sample processing and performed DNA extraction and library construction. M. Annala, L.R., J.N., J.V., and T. Virtanen performed computational and statistical data analysis. J.N., J.-P.M., T.T.S., T. Veitonmäki, L.M., M. Ahtiainen, and K.P. collected samples and clinical information. M. Annala, L.R., and J.N. wrote the manuscript. M. Annala, J.N., T.T.S., J.-P.M., and M.N. acquired funding. All authors discussed the results and participated in manuscript review and editing.

DECLARATION OF INTERESTS

M. Annala and J.V. are shareholders and employees of Fluivia. T.T.S. declares consultation fees from Tillots Pharma, Nouscom, and Mehiläinen; is CEO and co-owner of Healthfund Finland; and is a clinical advisory board member and minor shareholder of Lynsight.

STAR★METHODS

Detailed methods are provided in the online version of this paper and include the following:

- **KEY RESOURCES TABLE**
- **EXPERIMENTAL MODEL AND STUDY PARTICIPANT DETAILS**
 - Lynch syndrome-associated urothelial cancer tissue cohort
 - Urothelial cancer urine cohort
- **METHOD DETAILS**
 - Tissue DNA extraction and immunohistochemistry
 - Library construction and DNA sequencing
 - Sequence pre-processing and alignment
 - Somatic mutation analysis
 - Estimation of sample cancer fraction
- **QUANTIFICATION AND STATISTICAL ANALYSIS**

SUPPLEMENTAL INFORMATION

Supplemental information can be found online at <https://doi.org/10.1016/j.celrep.2025.116388>.

Received: March 26, 2025

Revised: August 6, 2025

Accepted: September 16, 2025

Published: October 3, 2025

REFERENCES

1. Ligtenberg, M.J.L., Kuiper, R.P., Chan, T.L., Goossens, M., Hebeda, K.M., Voorendt, M., Lee, T.Y.H., Bodmer, D., Hoenselaar, E., Hendriks-Cornelissen, S.J.B., et al. (2009). Heritable somatic methylation and inactivation of MSH2 in families with Lynch syndrome due to deletion of the 3' exons of TACSTD1. *Nat. Genet.* *41*, 112–117.
2. Møller, P., Seppälä, T.T., Bernstein, I., Holinski-Feder, E., Sala, P., Gareth Evans, D., Lindblom, A., Macrae, F., Blanco, I., Sijmons, R.H., et al. (2018). Cancer risk and survival in carriers by gene and gender up to 75 years of age: a report from the Prospective Lynch Syndrome Database. *Gut* *67*, 1306–1316.
3. Valo, S., Kaur, S., Ristimäki, A., Renkonen-Sinisalo, L., Järvinen, H., Mecklin, J.-P., Nyström, M., and Peltomäki, P. (2015). DNA hypermethylation appears early and shows increased frequency with dysplasia in Lynch syndrome-associated colorectal adenomas and carcinomas. *Clin. Epigenetics* *7*, 1–13.
4. Campbell, B.B., Light, N., Fabrizio, D., Zatzman, M., Fuligni, F., de Borja, R., Davidson, S., Edwards, M., Elvin, J.A., Hodel, K.P., et al. (2017). Comprehensive Analysis of Hypermutation in Human Cancer. *Cell* *171*, 1042–1056.e10.
5. Allory, Y., Beukers, W., Sagrera, A., Flández, M., Marqués, M., Márquez, M., van der Keur, K.A., Dyrskjot, L., Lurkin, I., Vermeij, M., et al. (2014). Telomerase reverse transcriptase promoter mutations in bladder cancer: high frequency across stages, detection in urine, and lack of association with outcome. *Eur. Urol.* *65*, 360–366.
6. Bell, R.J.A., Rube, H.T., Kreig, A., Mancini, A., Fouse, S.D., Nagarajan, R.P., Choi, S., Hong, C., He, D., Pekmezci, M., et al. (2015). Cancer. The transcription factor GABP selectively binds and activates the mutant TERT promoter in cancer. *Science* *348*, 1036–1039.
7. Borah, S., Xi, L., Zaug, A.J., Powell, N.M., Dancik, G.M., Cohen, S.B., Costello, J.C., Theodorescu, D., and Cech, T.R. (2015). Cancer. TERT promoter mutations and telomerase reactivation in urothelial cancer. *Science* *347*, 1006–1010.
8. Necchi, A., Madison, R., Pal, S.K., Ross, J.S., Agarwal, N., Sonpavde, G., Joshi, M., Yin, M., Miller, V.A., Grivas, P., et al. (2021). Comprehensive Genomic Profiling of Upper-tract and Bladder Urothelial Carcinoma. *Eur. Urol. Focus* *7*, 1339–1346.
9. Donahue, T.F., Bagrodia, A., Audenet, F., Donoghue, M.T.A., Cha, E.K., Sfakianos, J.P., Sperling, D., Al-Ahmadie, H., Clendenning, M., Rosty, C., et al. (2018). Genomic Characterization of Upper-Tract Urothelial Carcinoma in Patients With Lynch Syndrome. *JCO Precis. Oncol.* *2018*, PO.17.00143. <https://doi.org/10.1200/PO.17.00143>.
10. Nikkola, J., Ryyppö, L., Vuorinen, J., Kallio, H., Selin, H., Jämsä, P., Åkerla, J., Virtanen, T., Pekkarinen, T., Kaipia, A., et al. (2025). Sensitive Detection of Urothelial Cancer via High-volume Urine DNA Analysis. *Eur. Urol.* *87*, 86–88.
11. Joost, P., Therkildsen, C., Dominguez-Valentin, M., Jönsson, M., and Nilbert, M. (2015). Urinary tract cancer in Lynch syndrome; increased risk in carriers of MSH2 mutations. *Urology* *86*, 1212–1217.
12. Fujii, Y., Sato, Y., Suzuki, H., Kakiuchi, N., Yoshizato, T., Lenis, A.T., Mae-kawa, S., Yokoyama, A., Takeuchi, Y., Inoue, Y., et al. (2021). Molecular classification and diagnostics of upper urinary tract urothelial carcinoma. *Cancer Cell* *39*, 793–809.e8.
13. Suryo Rahmanto, Y., Jung, J.-G., Wu, R.-C., Kobayashi, Y., Heaphy, C.M., Meeker, A.K., Wang, T.-L., and Shih, I.-M. (2016). Inactivating ARID1A Tumor Suppressor Enhances TERT Transcription and Maintains Telomere Length in Cancer Cells. *J. Biol. Chem.* *291*, 9690–9699.

14. Heaphy, C.M., de Wilde, R.F., Jiao, Y., Klein, A.P., Edil, B.H., Shi, C., Bettegowda, C., Rodriguez, F.J., Eberhart, C.G., Hebbar, S., et al. (2011). Altered telomeres in tumors with ATRX and DAXX mutations. *Science* 333, 425.
15. Salari, K., Sundi, D., Lee, J.J., Wu, S., Wu, C.-L., DiFiore, G., Yan, Q.R., Pienkny, A., Lee, C.K., Oberlin, D., et al. (2023). Development and Multi-center Case-Control Validation of Urinary Comprehensive Genomic Profiling for Urothelial Carcinoma Diagnosis, Surveillance, and Risk-Prediction. *Clin. Cancer Res.* 29, 3668–3680.
16. Rabien, A., Rong, D., Rabenhorst, S., Schlomm, T., Labonté, F., Hofbauer, S., Forey, N., Le Calvez-Kelm, F., and Ecke, T.H. (2024). Diagnostic performance of Uromonitor and TERTpm ddPCR urine tests for the non-invasive detection of bladder cancer. *Sci. Rep.* 14, 30617.
17. Cercek, A., Lumish, M., Sinopoli, J., Weiss, J., Shia, J., Lamendola-Essel, M., El Dika, I.H., Segal, N., Shcherba, M., Sugarman, R., et al. (2022). PD-1 Blockade in Mismatch Repair-Deficient. *N. Engl. J. Med.* 386, 2363–2376.
18. Martin, M. (2011). Cutadapt removes adapter sequences from high-throughput sequencing reads. *EMBnet. J.* 17, 10–12.
19. Langmead, B., and Salzberg, S.L. (2012). Fast gapped-read alignment with Bowtie 2. *Nat. Methods* 9, 357–359.
20. Faust, G.G., and Hall, I.M. (2014). SAMBLASTER: fast duplicate marking and structural variant read extraction. *Bioinformatics* 30, 2503–2505.
21. Quinlan, A.R., and Hall, I.M. (2010). BEDTools: a flexible suite of utilities for comparing genomic features. *Bioinformatics* 26, 841–842.
22. Karczewski, K.J., Francioli, L.C., Tiao, G., Cummings, B.B., Alföldi, J., Wang, Q., Collins, R.L., Laricchia, K.M., Ganna, A., Birnbaum, D.P., et al. (2020). The mutational constraint spectrum quantified from variation in 141,456 humans. *Nature* 581, 434–443.
23. Wang, K., Li, M., and Hakonarson, H. (2010). ANNOVAR: functional annotation of genetic variants from high-throughput sequencing data. *Nucleic Acids Res.* 38, e164.

STAR★METHODS

KEY RESOURCES TABLE

REAGENT or RESOURCE	SOURCE	IDENTIFIER
Antibodies		
Mouse monoclonal anti-MLH1	Leica Biosystems	Clone ES05
Mouse monoclonal anti-MSH2	Calbiochem	Clone FE11
Rabbit monoclonal anti-MSH6	Epitomics	Clone EPR3945
Biological samples		
Formalin-fixed paraffin-embedded urothelial cancer tissue from patients with Lynch syndrome	Tampere Biobank, Helsinki Biobank, Auria Biobank, Central Finland Biobank, Eastern Finland Biobank, and Biobank Borealis of Northern Finland	N/A
Urine cell pellets from patients with sporadic urothelial cancer or Lynch syndrome associated urothelial cancer	Tampere University	N/A
Chemicals, peptides, and recombinant proteins		
Twist Library Preparation EF Kit 2.0	Twist Biosciences	104382
Twist Universal Adapter System – TruSeq compatible	Twist Biosciences	101308
IDT xGen Hybridization and Wash v2 Reagents	Integrated DNA Technologies	10010351
IDT xGen Hybridization and Wash v2 Beads	Integrated DNA Technologies	10010353
IDT xGen Exome hyb panel v2	Integrated DNA Technologies	10005151
UroScout custom xGen hybridization capture panel	Integrated DNA Technologies	N/A
QIAamp DNA FFPE Advanced UNG Kit	QIAGEN	56705
Deposited data		
Illumina targeted sequencing data	Tampere University	EGAD50000001220
Software and algorithms		
Bowtie	https://github.com/BenLangmead/bowtie2	Version 2.3.4.3
SAMBLASTER	https://github.com/GregoryFaust/samblaster	Version 0.1.24
Julia	https://github.com/JuliaLang/julia	Version 1.11.5
Mutato	https://github.com/annalam/mutato	Version 0.9.0

EXPERIMENTAL MODEL AND STUDY PARTICIPANT DETAILS

Lynch syndrome-associated urothelial cancer tissue cohort

A list of all patients, alive or deceased, with a Lynch syndrome diagnosis and histologically confirmed UC with clinical data available was obtained from the Finnish Lynch Syndrome Registry, regardless of sex, gender, race, or ethnicity. Formalin-fixed, paraffin-embedded (FFPE) urothelial cancer tissue samples available in six Finnish biobanks for these patients were collected. If a patient had tissue available from multiple surgeries or from multiple lesions during one surgery, all such samples were analyzed (but only one sample per tumor lesion). All patients provided written informed consent for the biobanking and utilization of their samples for research, and additional approval was obtained from all biobanks. Detailed information on the Lynch syndrome-associated urothelial cancer patient cohort is listed in [Table S1](#).

Urothelial cancer urine cohort

Patients were recruited to prospective urine collection between January 2021 and January 2024 at the Tampere University Hospital. All patients aged 18 years or older with a positive diagnostic cystoscopy, prior diagnosis of UC, or a cystoscopy referral for primary UC evaluation (due to hematuria or imaging findings) were invited to enroll, regardless of sex, gender, race, or ethnicity. The study was conducted in accordance with the Declaration of Helsinki, and the protocol was approved by the Regional Ethics Committee of Tampere University Hospital (identification code R21088B). All patients provided written informed consent before study participation.

Patients were instructed to collect 100 mL of first void urine (with a recommended minimum of 2 h since last urination) into a plastic cup at the Tampere University Hospital Urology Clinic or a sample bag at home. Patients added 5 mL of Streck Urine DNA preservative to the sample immediately after collection to ensure sample integrity at room temperature. Home urine samples were transported to Tampere University via standard mail.

METHOD DETAILS

Tissue DNA extraction and immunohistochemistry

All available slides per case were reviewed by a pathologist and re-classified according to WHO Classification of Tumors 5th edition. Representative cancerous areas and adjacent normal tissue (if available) on the 10 μm slides were identified and macrodissected using sterile scalpels, scraping tissue into 1.5 mL Eppendorf tubes. DNA was extracted from the macrodissected FFPE tissue using the QIAamp DNA FFPE Advanced UNG Kit, eluted in 17–40 μL of ATE buffer, and stored in -20C freezer. Immunohistochemical staining for MMR proteins used 4 μm slides. The slides were stained with antibodies for MLH1 (clone ES05, dilution 1:50; Novocastra, Leica Biosystems, Nussloch, Germany), MSH2 (FE-11, 1:50; Calbiochem, La Jolla, CA) and MSH6 (EPR3945, 1:150; Epitomics, Burlingame, CA) using a BOND-III Stainer and BOND Epitope Retrieval Solution 2 detection kit (Leica Biosystems). Based on nuclear staining in neoplastic cells, MMR protein expression was classified as lost or retained.

Library construction and DNA sequencing

Illumina DNA sequencing libraries were constructed from 24 to 100 ng of DNA using the Twist Enzymatic Fragmentation Library Prep Kit 2.0 with 7.5 min fragmentation time and following the manufacturer's recommended protocol. Sequencing libraries were multiplexed into pools, and target capture was carried out using custom IDT xGen hybridization capture panels and xGen Hybridization and Wash v2 Kit (IDT). The library pools were sequenced on an Illumina NovaSeq 6000 instrument using 2×150 bp paired end sequencing with v1.5 flow cells.

Sequence pre-processing and alignment

Adapters in read 3' ends were trimmed in paired end mode using cutadapt-1.11 with parameters $-m\ 20$ and $-a/-A\ AGATCGGAA-GAGC$.¹⁸ Reads were aligned against the hg38 reference genome using Bowtie-2.3.0 with parameters $-\text{max-ins}\ 1000\ -\text{score-min}\ L,0,-0.6$.¹⁹ Duplicate fragments were marked using samblaster-0.1.24 with default parameters and were omitted from further analyses.²⁰ Per-base read coverages in target regions were quantified using bedtools-2.25.0.²¹ Same-patient sample identities were verified based on single-nucleotide polymorphism (SNP) genotypes.

Somatic mutation analysis

To identify somatic mutations (base substitutions and indels) from UroScout targeted sequencing data from FFPE tumor tissue samples, we searched for variants with ≥ 7 supporting reads, allele fraction $\geq 5\%$, and allele fraction ≥ 20 times the background error rate in negative control samples. For mutations in urine tumor DNA samples, an allele fraction $\geq 1\%$ was required instead, given the lower rates of DNA damage in nuclear DNA extracted from urine cell pellets. To identify mutations in whole-exome sequenced FFPE tumor tissue samples, we searched for variants with ≥ 5 supporting reads, allele fraction $\geq 8\%$, and allele fraction ≥ 40 times the background error rate in negative control samples, to accommodate the lower sequencing depth and broader capture region. These mutation calling thresholds were halved for a curated set of 38 highly recurrent urothelial cancer mutations (Table S5).

For FFPE tissue samples sequenced using the UroScout assay, we quantified the position and allele specific background error rate based on negative control urine samples from 24 healthy volunteers (median age 39 years). For FFPE tissue samples sequenced with the whole-exome panel, we quantified background error rates based on a set of 20 adjacent normal FFPE tissue samples. We required that the average distance of the mutant allele from the nearest read end was ≥ 14 bases, and the average mapping quality of mutant allele carrying reads was ≥ 10 . Variants found in the gnomAD v3.0 germline variant database with a population frequency $\geq 0.5\%$ were discarded.²² Protein-level consequences of mutations were predicted using ANNOVAR.²³

Estimation of sample cancer fraction

We defined the cancer fraction of a tissue or urine sample as the fraction of genome equivalents in the sample originating from cancer cells, and used the formula $C = 2/(1/F + 1)$ to solve cancer fraction C based on the allele fraction F of each somatic mutation detected in the sample, and selected the highest cancer fraction estimate. This formula conservatively assumes loss-of-heterozygosity through deletion of the non-mutant allele.

QUANTIFICATION AND STATISTICAL ANALYSIS

Fisher's exact test and Mann–Whitney U test p -values were calculated using Julia (version 1.10.4) with the *HypothesisTests* package (version 0.11.0). The Benjamini-Hochberg procedure was used to correct for multiple hypothesis testing using the Julia package *MultipleTesting* (version 0.6.0).